

Atomic-scale self-organization of Co nanostructures embedded into Cu(100)

S. V. Kolesnikov, A. L. Klavsyuk, and A. M. Saletsky

Faculty of Physics, Moscow State University, Moscow 119991, Russian Federation

(Received 12 January 2009; revised manuscript received 26 February 2009; published 24 March 2009)

Formation of constrained nanostructures from Co atoms embedded within a Cu(100) surface is investigated on the atomic scale by performing molecular-dynamics and kinetic Monte-Carlo simulations. The atomic processes responsible for the linear and angular chain formations are identified. We demonstrate the key role of substrate vacancies in the motion of embedded Co atoms and investigate the self-organization of Co atoms in different conditions.

DOI: [10.1103/PhysRevB.79.115433](https://doi.org/10.1103/PhysRevB.79.115433)

PACS number(s): 61.46.–w

I. INTRODUCTION

Magnetic nanostructures are appealing for engineering of nanocomputers. During the past two decades Co nanosystems on copper surface had a special interest because of their unusual magnetic and electronic properties. The pioneering work of de la Figuera *et al.*¹ showed that Co thin film does not grow on Cu(111) surface layer by layer; it rather grows in the form of bilayer triangular islands. The magnetic properties of triangle nanoparticles with two monolayers height supported on Cu(111) surface were theoretically investigated.² Furthermore the unusual electronic properties of it was observed and explained by Diekhöner *et al.*³ Recently epitaxial growth of Co thin films on Cu(111) surface was simulated with kinetic Monte Carlo method.⁴ Ramsperger *et al.*⁵ investigated the growth of Co on stepped and flat Cu(100) surfaces and also found the deviation from layer by layer growth. In later works^{6,7} the magnetic and electronic properties of different stable and metastable structures were investigated and non-Arrhenius behavior of the island density was found. The process of bilayer Co islands formation was simulated by using accelerated molecular dynamics.⁸ The magnetic anisotropy of ultrathin Co/Cu(110) films was discovered by Hope *et al.*⁹ (see also Fassbender *et al.*¹⁰). In the recent works magnetic properties of Co nanorods grown on Cu(110) surface¹¹ and epitaxial growth of Co islands were explained.¹²

Moreover nanostructures can be built up from single atoms on the surface of metal with a scanning tunnel microscope (STM) tip,^{13,14} but with increasing temperature adatoms and small nanostructures would become unstable due to the thermally enhanced surface diffusion. On the other hand, the stability of many embedded structures is qualitatively understandable. It makes the idea to use a system with embedded atoms for nanostructuring very attractive. The more the diffusion mechanisms are understood at the atomic level, the more the fabrication processes can be controlled in order to obtain a better quality of the device performances. Therefore such structures are very appealing from the technological point of view.

In the past few years, the mobility of embedded atoms into a Cu(100) surface has been investigated with the usage of STM.^{15,16} Grant *et al.*¹⁵ investigated the kinetics of Pd/Cu alloys by following the motion of individual Pd atoms incorporated into a Cu(100) surface. The experiments of van Gas-

tel *et al.*¹⁶ showed the high mobility of In atoms embedded within the first layer of a Cu(100) surface. It has been demonstrated that surface vacancies are responsible for the mobility of the embedded atoms because they are always present in the surface. Mechanisms of vacancy motion were theoretically investigated by Montalenti *et al.*¹⁷ for Ag(100) surface and Boisvert and Lewis¹⁸ for Cu(100) surface. The self-organization and motion of vacancy clusters was simulated in the set of works.^{19–21} Atomic exchange processes for single adatoms and burrowing of clusters into the substrate have been investigated in several experiments and calculations even for metals immiscible in the bulk.^{22–24} Experiments of Kurnosikov *et al.*²⁵ showed the possibility to manipulate single atoms of Co embedded in to a Cu(001) surface with STM tip and to create in a controlled way small clusters which are stable at room temperature.

The main goal of our work is to investigate the evolution of Co nanostructures embedded into a Cu(100) surface at the atomic scale. The present calculations using the kinetic Monte Carlo (kMC) method with energy barriers of all relevant events calculated by means of the molecular-dynamics (MD) method with *ab initio* based interatomic potentials are performed.

The paper is organized as follows. In Sec. II, we briefly describe the MD-kMC model used for our simulations. In Sec. III, we concentrate on the main atomistic processes, responsible for evolution Co nanostructures, and present the results and discussions of the kMC simulations at different concentrations of Co atoms and surface vacancies. Conclusions are presented in Sec. IV.

II. COMPUTATIONAL METHOD

For the simulation of evolution of embedded atoms we apply a combination of MD and kMC methods. At the first stage we calculate all diffusion barriers in our model with MD method at zero temperature. To calculate diffusion barriers, we can describe Cu and Co atoms as classical particles which are interacting through interatomic potentials. In the present work, interatomic potentials are formulated in second moment of the tight-binding approximation.²⁶ In this approximation, the attractive term E_B^i (band energy) contains the many-body interaction. The repulsive part E_R^i is described by pair interactions (Born-Mayer form). The cohe-

sive energy E_C is the sum of the band energy and repulsive part

$$E_C = \sum_i (E_R^i + E_B^i), \quad (1)$$

$$E_B^i = - \left\{ \sum_j \xi_{\alpha\beta}^2 \exp \left[-2q_{\alpha\beta} \left(\frac{r_{ij}}{r_0^{\alpha\beta}} - 1 \right) \right] \right\}^{1/2}, \quad (2)$$

$$E_R^i = \sum_j \left[A_{\alpha\beta}^1 \left(\frac{r_{ij}}{r_0^{\alpha\beta}} - 1 \right) + A_{\alpha\beta}^0 \right] \exp \left[-p_{\alpha\beta} \left(\frac{r_{ij}}{r_0^{\alpha\beta}} - 1 \right) \right], \quad (3)$$

where r_{ij} is distance between the atoms i and j , α and β are types of atoms, $\xi_{\alpha\beta}$ is an effective hopping integral, $p_{\alpha\beta}$ and $q_{\alpha\beta}$ describe the decay of the interaction strength with distance between atoms, and $r_0^{\alpha\beta}$, $A_{\alpha\beta}^0$, and $A_{\alpha\beta}^1$ are adjustable parameters of interatomic interaction.²⁷ The interatomic potentials reproduce the bulk properties of Cu and Co crystals and the *ab initio* calculated properties of supported and embedded Co clusters. The details of the fitting procedure are described in Ref. 28. Reliability of our potentials for different atomic structures (single adatoms, supported clusters, embedded clusters, nanocontacts) has been demonstrated.^{29–31}

In our model we consider diffusion of embedded atoms only through exchanges with surface vacancies. A concentration of the vacancies is not high so, for accelerating our calculations at the kMC stage, we suppose that only surface vacancies can be moved. In the framework of our MD-kMC model we consider all possible processes: Co-vacancy and Cu-vacancy exchanges in the first layer of copper substrate. The diffusion barriers of vacancies are computed by means of the MD, where the positions of Co and Cu atoms are determined in fully relaxed geometry. The slab consists of eight layers with 2000 atoms in each layer. Two bottom layers are fixed and periodic boundary conditions are applied in the surface plane. The cutoff radius for the interatomic potentials is set to 6.0 Å.

At the second stage of our investigation we employ the general kMC method. The kMC model was developed by Voter and co-workers^{32,33} and was used in several recent studies.^{4,12,34–36} According to this approach the frequency ν_i of the vacancy transition is calculated as

$$\nu_i = \nu_0 \exp \left(- \frac{E_i^D}{kT} \right), \quad (4)$$

where E_i^D is the diffusion barrier, T is the copper substrate's temperature, k is the Boltzmann constant, and ν_0 is the prefactor. Generally ν_0 and E_i^D are functions of the surface temperature. However, Kürpick and Rahman³⁷ showed that frequency prefactor ν_0 is constant in the range of 200–600 K for processes in the first layer of Cu(100) surface. Moreover, the diffusion barriers \tilde{E}_i^D at finite temperature ($T < 600$ K) for such processes differ from diffusion barriers E_i^D at zero temperature no more than 10%. Thus, we use the approach (4) with diffusion barriers E_i^D calculated at zero temperature and for all considered processes we take ν_0 as 10^{12} Hz.^{34,35}

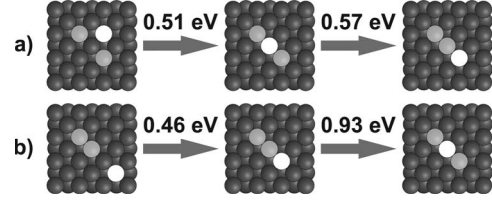


FIG. 1. Transitions responsible for the (a) association and (b) dissociation of Co dimers. Dark-gray, light-gray, and white represent Cu atoms, Co atoms, and vacancies, respectively.

For increasing of clearness of our statements relative probabilities of complex processes will be considered. Because the vacancy in the Cu(100) surface can move in four different directions the probability of the simple event is calculated as

$$p_i = \frac{\nu_i}{\sum_{j=1}^4 \nu_j}, \quad (5)$$

then the probability of the complex process is the multiplication of the simple event's probabilities. For more correct calculations we use random number generator from the book.³⁸

III. RESULTS AND DISCUSSIONS

In this section, we concentrate on the formation of linear and angular chains from embedded Co atoms. We discuss basic atomic processes, responsible for forming these structures, and present the results of kMC simulations.

At first, we need to understand how embedded Co atoms can travel in the copper surface at 300–400 K. The Co-Cu exchange in the Cu(100) surface is nearly impossible because exchange barrier is enormous (2.13 eV). However, first layer of the copper surface always contains some concentration of vacancies. The barrier of vacancy diffusion (vacancy-Cu exchange) is only 0.34 eV, so vacancies in the Cu(100) surface are very mobile: $\tau_{\text{vac}}^{\text{diff}} = 5.9 \times 10^{-7}$ s at 300 K and $\tau_{\text{vac}}^{\text{diff}} = 2.1 \times 10^{-8}$ s at 400 K. Summarizing these statements, we assume that embedded Co atoms' diffusion can be realized mainly via Co-vacancy exchanges.

To understand the mechanism of nanostructures formation on the atomic scale, we consider the dominant processes leading to Co atoms' movement and estimate the probabilities of these processes. For single Co atom diffusion two events are necessary: hop of the vacancy toward the Co atom with barrier of 0.46 eV and the Co-vacancy exchange with a barrier of 0.59 eV. The total probability of this process is 3.6×10^{-6} at 300 K and 8.5×10^{-5} at 400 K.

Figure 1 demonstrates the formation and dissociation of dimers. When two single Co atoms meet each other, the formation of dimer [Fig. 1(a)] takes place through two stages: the vacancy disposes side by side with both Co atoms with a barrier of 0.51 eV and Co-vacancy exchange happens with a barrier of 0.57 eV. The total probability of the dimer formation p_1 is 2.1×10^{-7} at 300 K and 9.8×10^{-6} at 400 K. The

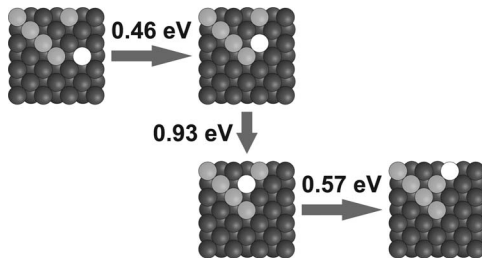


FIG. 2. Transitions responsible for the association of the Co atom to inner atoms of the linear Co chain. Dark-gray, light-gray and white represent Cu atoms, Co atoms, and vacancies, respectively.

dissociation of dimer [Fig. 1(b)] is less operative because of the big diffusion barrier of 0.93 eV at the second stage. The total probability of this process $p_{\text{dis}} \approx 10^{-3}p_1$ at 400 K.

Now, we consider trimer formation from embedded Co atoms. At low concentration of Co atoms this process is similar to dimer formation: it proceeds in two stages with barriers of 0.51 and 0.57 eV consequently. The probability of linear trimer formation is $p_1/2$. The probability of angular trimer formation is p_1 if the axis of dimer has been perpendicular to the direction of monomer's jumping and $p_1/2$ if the axis of dimer has been parallel to the direction of the adatom's hopping. Another situation takes place at high concentration of alloy when meeting of three single Co atoms is possible: the vacancy is placed between three Co atoms with a barrier of 0.56 eV and Co-vacancy exchange happens with a barrier of 0.27 eV. The probability of this process is significantly higher than the analogous probability at low concentration of Co atoms $p \approx 100p_1$ at 400 K. At the same time, the probability of angular trimer formation is twice higher than probability of linear trimer formation.

Hence, the formation of two types of Co chains is possible: linear and angular chains. We discuss the mechanisms of associating single Co atoms with each type of Co chains. First, we concentrate on the behavior of the Co monomers close to the linear chain. Further, we proceed to the behavior of the Co atoms near the zigzag chain, the simplest example of the angular chain.

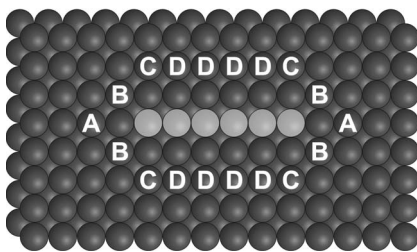


FIG. 3. Different positions of a single Co atom before association with the linear Co chain. Formation of a linear chain takes place with the probability of $p_1/2$ if the Co monomer is in the A or B positions. Formation of an angular chain takes place with the probability of $p_1/2$ if the Co monomer is in the B position or p_1 if the Co monomer is in the C position. If the single Co atom is in the D position it can associate with an inner atom of the chain with probability of $10^{-3}p_1$ at 400 K. Dark-gray and light-gray represent Cu and Co atoms, respectively; $p_1 = 9.8 \times 10^{-6}$ at 400 K.

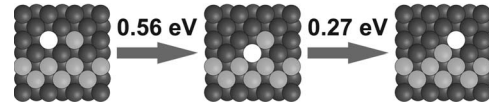


FIG. 4. Transitions responsible for the association of the Co atom to inner atoms of the zigzag Co chain. Dark-gray, light-gray, and white represent Cu atoms, Co atoms, and vacancies, respectively.

Figures 2 and 3 clarify how single Co atoms associate with the linear Co chain. The process of single Co atom association to inner atoms in the chain (Fig. 2) consists of three consecutive events: a vacancy hops toward the chain with a barrier of 0.46 eV, dislocates between the single Co atom and the inner atom of the chain with a barrier of 0.93 eV, and makes an exchange with the Co monomer with a barrier of 0.57 eV. The probability of this complex process is $p \approx 10^{-3}p_1$ at 400 K. On the other hand, the process of single Co atom association to the edge of the chain is similar to trimer formation. Thus, Co atoms associate mainly to the edge of the linear Co chains. Figure 3 summarizes our findings about the probabilities of Co monomer association with the linear Co chain and demonstrates that formation of angular chains is twice probable than formation of linear chains. Finally, we need to note that the process of Co atom transition along the chain is unlikely at 400 K because of a high Co-vacancy exchange barrier (0.93 eV).

The process of single Co atom association to inner atoms of the zigzag Co chain (Fig. 4) is simpler and more probable than in the case of the linear chains. A vacancy dislocates between two atoms of the zigzag chain and the Co monomer with a barrier of 0.56 eV, then Co-vacancy exchange takes place with a low barrier (0.27 eV). This process has a probability $p \approx 100p_1$ at 400 K. Whereas, the process of single Co atom association to the edge of the zigzag Co chain is similar to association to the edge of linear chain.

The process of 2×2 cluster formation is similar to association of the Co atom to the inner atoms of the zigzag chain and has a probability $p \approx 100p_1$ at 400 K. Further association of Co monomers to the 2×2 cluster is similar to trimer formation and its probability is $p = p_1$ or $p = p_1/2$ depending on the initial displacement of the monomer and the 2×2 cluster.

As it has been mentioned above, vacancies in the first layer of Cu(100) surface are very mobile and that leads to the formation of compact clusters from the vacancies. The vacancies spend the most part of their time in the vacancy cluster, but if the vacancy locates on the edge of the cluster it can leave the cluster through hops in the direction out of the edge: the first jump has a barrier of 0.43 eV and second jump has a barrier of 0.34 eV. We suppose that the existence and displacement of the vacancy cluster does not depend on further jumps of the vacancy until the vacancy approaches to the cluster again on the distance less than two neighbor's distance. The probability of leaving vacancy cluster is $p_{\text{leave}}^{\text{vac}} = 1.5 \times 10^{-4}$ at 300 K and $p_{\text{leave}}^{\text{vac}} = 1.8 \times 10^{-3}$ at 400 K. Thus, the mean time of the process is proportional to $\tau_{\text{vac}}^{\text{diff}} / (p_{\text{vac}}^{\text{process}} p_{\text{leave}}^{\text{vac}})$. This simple ratio can be used for comparison of mean times of some processes at different tem-

peratures; for instance, the mean time of Co monomer's diffusion at 300 K is 7800 times longer than at 400 K.

From our MD investigation we can make the following conclusions: (i) The main time of embedded Co atom's diffusion at 400 K is significantly less than at 300 K, thus evolution of the investigated system accelerates with increasing of copper substrate's temperature, and the formation of constrained structures from Co atoms in the first layer of Cu(100) surface at 400 K is possible. (ii) If during the process of evolution the linear chain from N cobalt atoms has formed ($N > 2$), then the probability of association of the single Co atom to one of the $N-2$ inner atoms of the chain is significantly less than the probability of association to the outer atoms of the chain. Consequently, the formation of such compact structures as square clusters bigger than 2×2 during the evolution is highly unlikely. (iii) If during the process of evolution the constrained structure from N embedded Co atoms has been formed, then this structure is linear chain with a probability of 3^{2-N} . Thus, with increasing of Co concentration, in general, angular structures are formed.

Now, we discuss the results of our kMC simulations. It is necessary to note that at temperatures higher than 400 K processes of vacancy appearing and covering of Co atoms with atoms of the substrate take place. On the other hand, our kMC investigation shows that at temperatures lower than 400 K the mobility of embedded Co atoms decreases and compact structures in the Cu(100) surface cannot be formed. Consequently, the formation of constrained Co nanostructures without being covered with copper atoms is realized only in narrow range of temperatures near 400 K.

At the Fig. 5 the results of our simulations for cases of low and high concentrations of Co alloy at 400 K are presented. In contradiction to the case of Co atoms self-organization on the Cu(100) surface,⁸ embedded Co atoms do not gather into compact clusters and the angular structures are formed. The increase of Co atoms concentration infers to the result of self-organization of Co atoms: the number of simple structures is decreasing and the number of complex structures is increasing.

It can be noted that a concentration of substrate vacancies N_v does not infer to result pattern of evolution, but the speed of the evolution depends on the vacancy concentration. It has been discussed before that vacancies form the rectangular clusters and the probability of leaving the cluster is not high.

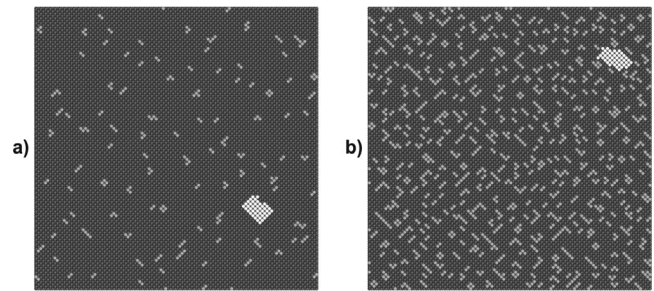


FIG. 5. kMC simulations of surface morphology at the different concentrations of embedded Co atoms: (a) $n_{\text{Co}}=0.0375$ ML, (b) $n_{\text{Co}}=0.1875$ ML. Other parameters of the simulations are the same: $T=400$ K, $n_{\text{vac}}=0.00625$ ML. Dark-gray, light-gray, and white represent Cu atoms, Co atoms, and vacancies, respectively. The area 21.7×21.7 nm² is demonstrated.

On the other hand, a free vacancy can join back to the vacancy cluster with a probability which is proportional to the perimeter of the cluster. So, the total time of compact structures formation is approximately proportional to $\sqrt{N_v}$. This estimation agrees with our kMC simulations.

IV. CONCLUSION

In summary, we have performed atomic-scale simulations of the self-organization of Co atoms embedded into a Cu(100) surface. We have shown that the motion of embedded Co atoms is the result of an intensive diffusion of substrate vacancies. The major atomic events responsible for the formation of embedded Co nanostructures have been identified. We have revealed that during the process of evolution, in general, angular structures are formed. The temperature conditions of such scenario of self-organization have been determined and the influence of Co atom's concentration and vacancy's concentration to evolution of the system has been analyzed.

ACKNOWLEDGMENTS

We would like to thank N. N. Negulyaev for valuable discussions concerning the kMC method. Computational resources were provided by Research Computing Center of the Moscow State University (MSU NIVC).

¹J. de la Figuera, J. E. Prieto, C. Ocal, and R. Miranda, Phys. Rev. B **47**, 13043 (1993).

²J. Izquierdo, A. Vega, and L. C. Balbás, Phys. Rev. B **55**, 445 (1997).

³L. Diekhöner, M. A. Schneider, A. N. Baranov, V. S. Stepanyuk, P. Bruno, and K. Kern, Phys. Rev. Lett. **90**, 236801 (2003).

⁴N. N. Negulyaev, V. S. Stepanyuk, P. Bruno, L. Diekhöner, P. Wahl, and K. Kern, Phys. Rev. B **77**, 125437 (2008).

⁵U. Ramsperger, A. Vaterlaus, P. Pfäffli, U. Maier, and D. Pescia, Phys. Rev. B **53**, 8001 (1996).

⁶R. Pentcheva and M. Scheffler, Phys. Rev. B **61**, 2211 (2000).

⁷R. Pentcheva, K. A. Fichthorn, M. Scheffler, T. Bernhard, R. Pfandzelter, and H. Winter, Phys. Rev. Lett. **90**, 076101 (2003).

⁸R. A. Miron and K. A. Fichthorn, Phys. Rev. B **72**, 035415 (2005).

⁹S. Hope, E. Gu, M. Tselepi, M. E. Buckley, and J. A. C. Bland, Phys. Rev. B **57**, 7454 (1998).

¹⁰J. Fassbender, G. Güntherodt, C. Mathieu, B. Hillebrands, R. Jungblut, J. Kohlhepp, M. T. Johnson, D. J. Roberts, and G. A. Gehring, Phys. Rev. B **57**, 5870 (1998).

- ¹¹X. D. Ma, T. Nakagawa, Y. Takagi, M. Przybylski, F. M. Leibsle, and T. Yokoyama, *Phys. Rev. B* **78**, 104420 (2008).
- ¹²O. V. Stepanyuk, N. N. Negulyaev, A. M. Saletsky, and W. Hergert, *Phys. Rev. B* **78**, 113406 (2008).
- ¹³H. C. Manoharan, C. P. Lutz, and D. M. Eigler, *Nature (London)* **403**, 512 (2000).
- ¹⁴M. F. Crommie, *J. Electron Spectrosc. Relat. Phenom.* **109**, 1 (2000).
- ¹⁵M. L. Grant, B. S. Swartzentruber, N. C. Bartelt, and J. B. Hannon, *Phys. Rev. Lett.* **86**, 4588 (2001).
- ¹⁶R. van Gastel, E. Somfai, S. B. van Albada, W. van Saarloos, and J. W. M. Frenken, *Phys. Rev. Lett.* **86**, 1562 (2001); *Surf. Sci.* **521**, 10 (2002).
- ¹⁷F. Montalenti, A. F. Voter, and R. Ferrando, *Phys. Rev. B* **66**, 205404 (2002).
- ¹⁸C. Boisvert and L. J. Lewis, *Phys. Rev. B* **56**, 7643 (1997).
- ¹⁹K. Morgenstern, E. Lægsgaard, and F. Besenbacher, *Phys. Rev. B* **66**, 115408 (2002).
- ²⁰L. Niebergall, G. Rodary, H. F. Ding, D. Sander, V. S. Stepanyuk, P. Bruno, and J. Kirschner, *Phys. Rev. B* **74**, 195436 (2006).
- ²¹Y. Shim, V. Borovikov, B. P. Uberuaga, A. F. Voter, and J. G. Amar, *Phys. Rev. Lett.* **101**, 116101 (2008).
- ²²J. Fassbender, R. Allenspach, and U. Dürig, *Surf. Sci.* **383**, L742 (1997).
- ²³C. G. Zimmermann, M. Yeadon, K. Nordlund, J. M. Gibson, R. S. Averback, U. Herr, and K. Samwer, *Phys. Rev. Lett.* **83**, 1163 (1999); S. Padovani, F. Scheurer, and J. P. Bucher, *Europhys. Lett.* **45**, 327 (1999).
- ²⁴F. Nouvertne, U. May, M. Bamming, A. Rampe, U. Korte, G. Guntherodt, R. Pentcheva, and M. Scheffler, *Phys. Rev. B* **60**, 14382 (1999); V. S. Stepanyuk, D. V. Tsivline, D. I. Bazhanov, W. Hergert, and A. A. Katsnelson, *ibid.* **63**, 235406 (2001); R. C. Longo, V. S. Stepanyuk, W. Hergert, A. Vega, L. J. Gallego, and J. Kirschner, *ibid.* **69**, 073406 (2004).
- ²⁵O. Kurnosikov, J. T. Kohlhepp, and W. J. M. de Jonge, *Europhys. Lett.* **64**, 77 (2003); *Surf. Sci.* **566-568**, 175 (2004).
- ²⁶F. Cleri and V. Rosato, *Phys. Rev. B* **48**, 22 (1993).
- ²⁷The potentials are used in the form of Ref. 26. The parameters are the following: for Cu-Cu, $A^1=0.0$ eV, $A^0=0.0854$ eV, $\xi=1.2243$ eV, $p=10.939$, $q=2.2799$, and $r_0=2.5563$ Å; for Co-Cu, $A^1=-1.5520$ eV, $A^0=-0.0372$ eV, $\xi=0.8522$ eV, $p=7.6226$, $q=5.5177$, and $r_0=2.4995$ Å; for Co-Co, $A^1=0.0$ eV, $A^0=0.1209$ eV, $\xi=1.5789$ eV, $p=11.3914$, $q=2.3496$, and $r_0=2.4953$ Å.
- ²⁸N. A. Levanov, V. S. Stepanyuk, W. Hergert, D. I. Bazhanov, P. H. Dederichs, A. A. Katsnelson, and C. Massobrio, *Phys. Rev. B* **61**, 2230 (2000).
- ²⁹V. S. Stepanyuk, A. L. Klavsyuk, L. Niebergall, A. M. Saletsky, W. Hergert, and P. Bruno, *Phase Transitions* **78**, 61 (2005).
- ³⁰S. Pick, V. S. Stepanyuk, A. L. Klavsyuk, L. Niebergall, W. Hergert, J. Kirschner, and P. Bruno, *Phys. Rev. B* **70**, 224419 (2004).
- ³¹V. S. Stepanyuk, A. L. Klavsyuk, W. Hergert, A. M. Saletsky, P. Bruno, and I. Mertig, *Phys. Rev. B* **70**, 195420 (2004).
- ³²A. F. Voter, *Phys. Rev. B* **34**, 6819 (1986).
- ³³A. F. Voter, F. Montalenti, and T. C. Germann, *Annu. Rev. Mater. Res.* **32**, 321 (2002).
- ³⁴A. Bogicevic, J. Strömquist, and B. I. Lundqvist, *Phys. Rev. Lett.* **81**, 637 (1998).
- ³⁵S. Ovesson, A. Bogicevic, and B. I. Lundqvist, *Phys. Rev. Lett.* **83**, 2608 (1999).
- ³⁶K. A. Fichthorn and M. Scheffler, *Phys. Rev. Lett.* **84**, 5371 (2000); M. Muller, K. Albe, C. Busse, A. Thoma, and T. Michely, *Phys. Rev. B* **71**, 075407 (2005).
- ³⁷U. Kürpick and T. S. Rahman, *Phys. Rev. B* **59**, 11014 (1999).
- ³⁸Numerical recipes in FORTRAN90. www.physics.louisville.edu/help/nr/bookf90pdf.html